Applied Catalysis B: Environmental 84 (2008) 524–532

Contents lists available at ScienceDirect

Applied Catalysis B: Environmental

journal homepage: www.elsevier.com/locate/apcatb

Photocatalytic reactions of imazamox at TiO_2, H_2O_2 and TiO_2/H_2O_2 in water interfaces: Kinetic and photoproducts study

M. Harir [a,d,*], A. Gaspar [a], B. Kanawati [a], A. Fekete [a], M. Frommberger [a], D. Martens [b], A. Kettrup [c], M. El Azzouzi [d], Ph. Schmitt-Kopplin [a,*]

[a] Helmholtz Center Munich, Research Center for Environmental Health, Institute of Ecological Chemistry, Ingoldstädter Landstraße 1, D-85764 Neuherberg, Germany
[b] LUFA, Obere Langgasse 40, 67346 Speyer, Germany
[c] Rumbecker Höhe 10, 59821 Arnsberg, Germany
[d] University Mohamed V-Agdal, Faculty of Sciences, Av. Ibn Batouta, BP 1014 Rabat, Morocco

ARTICLE INFO

Article history:
Received 1 June 2007
Received in revised form 13 May 2008
Accepted 13 May 2008
Available online 23 May 2008

Keywords:
Photodegradation
Imazamox
Oxidation
Kinetics
Photo-products
DFT

ABSTRACT

The photocatalytic transformation of imazamox, a herbicide of imidazolinone family, is investigated in aqueous solution containing titanium dioxide, hydrogen peroxide or the combination of TiO_2/H_2O_2 under simulated sunlight irradiation. The effect of parameters such as the amount of catalysts, the concentration of herbicide, and the pH were investigated by measurement of the rate constant of degradation. Experimental data obtained under different conditions describe the dependency of degradation rate on the above mentioned parameters. Consequently, kinetic parameters were experimentally determined and a pseudo-first-order kinetic was observed. Mulliken charge distributions calculated by the DFT method B3LYP/6–31+G(d) level of theory for key cationic, anionic and neutral structures of imazamox give interpretation for the dependency of photodegradation rate constant on pH. The degradation rate constants were always higher for the heterogeneous catalysis in reactions (TiO_2/UV, TiO_2/UV/H_2O_2) compared to the homogeneous systems (UV alone, H_2O_2/UV). In parallel, five photoproducts could be tentatively identified using Electrospray ionization Fourier transform ion cyclotron resonance mass spectroscopy based on precise chemical formula assignments.

© 2008 Elsevier B.V. All rights reserved.

1. Introduction

Light has been used in the chemical treatment of water since many years. In all cases, direct action of light is limited due to the absorption spectra of pollutants to be degraded. Thus, direct photochemical reaction has given a way to a sensitized photochemical or photoassisted reaction via introduction of compounds such as H_2O_2 [1–4] or ozone [5,6], that allow the formation of oxidizing species such as $^{\bullet}OH$ radicals. Hence, the complete photo-oxidation of organic compounds has been reported in many examples. The photocatalytic degradation of 22 organic substances was studied in titanium dioxide aqueous suspension [7,8] and over immobilized titanium dioxide thin films [9,10]. The photomineralization [11] and photodegradation [12] of halogenated organic pollutants were also investigated. It is known that the photocatalyst TiO_2 is first excited by UV light and subsequently initiates the photodegradation process. TiO_2 particles absorb light and generate electron/hole pairs (Eq. (1)).

$$TiO_2 + h\nu \rightarrow TiO_2(e_{cb}^- + h_{vb}^+) \quad (1)$$

The holes (h^+) in valence band are subsequently trapped by OH^- ions or H_2O to yield $^{\bullet}OH$ radicals (Eq. (2)), while the electrons (e^-) in the conduction band are trapped by preadsorbed O_2 molecules to yield superoxide radicals $O_2^{\bullet -}$ species which can interact with protons to generate $^{\bullet}OOH$ radicals (Eqs. (3a) and (3b)) [13]:

$$h^+ + H_2O(\text{or } OH^-) \rightarrow {}^{\bullet}OH + H^+(\text{or}\,{}^{\bullet}OH) \quad (2)$$

$$e_{cb}^- + O_2 \rightarrow O_2^{\bullet -} \quad (3a)$$

$$O_2^{\bullet -} + H^+ \rightarrow {}^{\bullet}OOH \quad (3b)$$

The hole, $^{\bullet}OH$ and $^{\bullet}OOH$ have strong oxidation activity. They can oxidize and even completely mineralize almost all of organic compounds. In the suspension, $^{\bullet}OH$ and/or $^{\bullet}OOH$ radicals play a major role in the photocatalytic oxidation, while the electron/hole pairs may also directly react with organic substrate on the surface [14].

* Corresponding author.
E-mail address: mourad.harir@helmholtz-muenchen.de (M. Harir).

0926-3373/$ – see front matter © 2008 Elsevier B.V. All rights reserved.
doi:10.1016/j.apcatb.2008.05.010

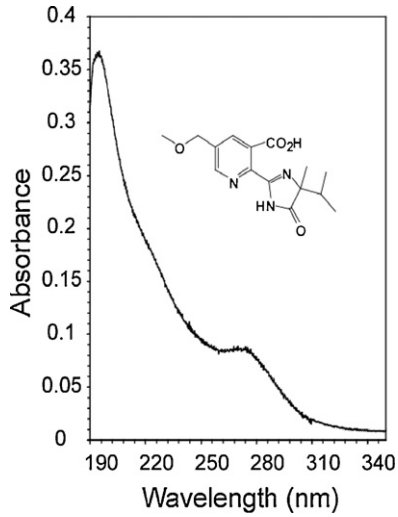

Fig. 1. Absorbance spectra of aqueous solutions (0.065 mM) of imazamox at pH 7. The structure of the herbicide is also reported.

Of the chemicals likely to be found in groundwater, pesticides have a non-negligible presence and their elimination is necessary, especially if the water is to be used for human life consumption. We are therefore working on this class of pollutants, and the present study concerns one herbicide in particular: imazamox 2-[4,5-dihydro-4-methyl-4-(1-methylethyl)-5-oxo-1H-imidazol-2-yl]-5-(methoxymethyl)-3-pyridinecarboxylic acid (Fig. 1), a herbicide from imidazolinone family which inhibits the enzyme plant acetohydroxyacid synthase, interferes with DNA, protein synthesis and disrupts cell growth, persist in the soil and may cause injury to crops planted in the following year.

Several studies reported the photolysis and photocatalysis degradation of imidazolinone [15–25]. However, no previous work reported a full investigation of the photocatalytic degradation of imazamox. In the present work, the photochemical degradation of imazamox was investigated with combination of theoretical calculations which bring more insight on the structures of imazamox under different pH conditions. This study was performed in order to compare the efficiency of different photocatalytic degradation processes in the presence of UV, TiO_2, or H_2O_2 only and their combinations. To define the main photoproducts, Electrospray ionization Fourier transform ion cyclotron resonance-mass spectroscopy analysis is used as an effective tool for characterization of the photo-degradation products.

2. Experimental

2.1. Materials

Imazamox, Purity >99%, was purchased from Dr. Ehrenstorfer, Germany, and used without further purification. Hydrogen peroxide (30%) and Titanium dioxide P-25 (mainly anatase ca. 50 $m^2\,g^{-1}$ nonporous) were purchased from (Aldrich, Germany). HPLC solvents were chromatography grade and all other chemicals were analytical grade and were used without further purification. Ultra pure water was produced with a MilliQ system (Millipore, Billerica, MA, USA). For photodegradation studies, phosphate buffers (KH_2PO_4 and K_2HPO_4), purchased from Aldrich, Germany were used. The solutions were initially buffed at pH 7.0 and then the pH were adjusted by addition of NaOH (small pastilles) or H_3PO_4.

2.2. Photoreactor

A cylindrical Pyrex glass vessel of 250 ml was used as a batch reactor. Solar irradiation was simulated by using a Suntest apparatus from Heraeus (Hanau, Germany) equipped with a Xenon lamp; UV-B (280 to 320 nm), 2.71 W/m^2 and UV-A (320 to 400 nm), 58.0 W/m^2). The emission spectrum between 400 and 800 nm follows the solar spectrum. The UV radiation is limited at 280 nm and the illuminance is approximately 150 k Lux.

2.3. Kinetic experiments

The solution was stirred 30 min in the dark with magnetic stirrer (before starting the irradiation experiment) to homogenize the medium. Fifty millilitre of aqueous solutions of imazamox ($C = 19.67 \times 10^{-2}$ mM) were exposed to photodegradation at different irradiation times. The irradiation experiments were performed at 30 °C and samples were collected at regular times and analysed directly after filtration (SPARATAN Filter 13/0.2RC; 0.2 μm; Schleichter & Schuell MicroScience, Germany) by HPLC coupled to Diode Array UV detector (without pre-concentration). Hydrolysis experiments were also performed at the same time as the photolysis study and no hydrolysis effect was observed.

2.4. Instrumentation and conditions used

HPLC was performed using a Perkin-Elmer Series 200 equipped with a diode array detector 235C (Wellesley, MA, USA). A LiChrospher100 RP-18 column (250 mm × 4 mm i.d., 5 μm) was used for the imazamox disappearance kinetic studies and the flow rate of isocratic elution (water pH3.0/acetonitrile; 80/20; v/v) was 0.9 ml/min.

All FT-ICR-MS experiments were carried out on an APEX Qe Fourier transform ion cyclotron resonance mass spectrometer (Bruker, Bremen, Germany) equipped with a 12 T superconducting magnet and Apollo I ESI source. For the positive electrospray measurements, the samples were diluted in methanol (1/1, v/v) and then introduced into the microelectrospray source at a flow rate of 120 μl/h with a nebulizer gas pressure of 20 psi and a drying gas pressure of 15 psi (250 °C). The voltage difference between the Electrospray needle and the counter electrode in the ESI ion source was 3.5 kV. Spectra were externally calibrated on clusters of arginine (10 ppm in methanol); calibration errors in the relevant mass range were always below 0.1 ppm. The spectra were acquired with a time domain size of 1 Megaword, which represents sufficient data points for each acquisition. The mass range used is m/z = 100–600. The ion accumulation number was set to 128 scans for each acquisition.

2.5. Mass measurement calculations

FT-ICR mass spectra were exported to peak lists. From those lists, possible elemental formulas were calculated for each peak in batch mode by a home-made software. The generated formulas were validated by setting sensible chemical constraints (Nitrogen rule, O/C ratio ≤ 1, H/C ratio $\leq 2n + 2$, element counts: $C \leq 20$, $H \leq 30$, $O \leq 6$, $N \leq 4$) in conjunction with an automated theoretical isotope pattern comparison. From the generated formulas, around five possible photoproducts could be identified from the analyzed mixture.

2.6. Theoretical calculations of the structures and Mulliken charge distributions

The electronic structure calculations were performed on a stand-alone computer using Density Functional Theory, incorporated in

Gaussian 03W program [26]. The hybrid DFT method B3LYP was implemented. All geometry optimizations were performed using 6–31+G(d) basis set. Frequency calculations were also done for each optimized geometry using the same basis set 6–31+G(d) to confirm that each optimized geometry does represent an energy minimum structure (not a transition state). The use of diffuse functions was important to represent the correct geometry of anionic and cationic species. Stability tests on all calculated structures were performed to ensure that the used wave function does represent the lowest energy solution of the self consistent field SCF equations.

For geometry optimization, the Berny [27] analytical gradient optimization routines were used in combination with the GDIIS algorithm [28–30]. The requested convergence in the density matrix was 10^{-8}, the threshold value for maximum displacement was 0.0018 Å, and that for the maximum force was 0.00045 Hartree/Bohr. All geometries of electronic structures calculated were rendered by Gauss View program [31]. Mulliken charge distribution was calculated for each optimized structure on the B3LYP/6–31+G(d) level of theory.

3. Results and discussion

3.1. Preliminary kinetic of imazamox disappearance

In order to observe the effect of the photocatalyst and UV light on imazamox degradation, the herbicide was photochemically degraded under UV, TiO_2, or H_2O_2 only and by using their various combinations. Under UV irradiation without any additive, the reduction of imazamox concentration was less than 5% after 15 min of irradiation (Fig. 2a). When H_2O_2 was added, the reduction of imazamox concentration was enhanced slightly to reach 11% after 15 min (Fig. 2b). After 1 h of photolysis, the difference of the percental reduction amount of imazamox between experiment (a) and (b) (Fig. 2) increased to 38%. This effect could be attributed to the direct photolysis of H_2O_2 results in formation of OH radicals [32]. On the other hand, in heterogeneous photocatalysis (Fig. 2c and 2d) the mechanism of the semiconductor-catalyzed oxidative degradation of organic compounds in aqueous systems can be explained by the band-gap model [32].

$$H_2O_2 + h\nu \rightarrow 2^{\bullet}OH \quad (4)$$

$$TiO_2 + h\nu \rightarrow TiO_2(e^- + h^+) \quad (5)$$

$$TiO_2(h^+) + RX_{ad} \rightarrow TiO_2 + RX_{ad}^{\bullet +} \quad (6)$$

$$TiO_2(h^+) + H_2O_{ad} \rightarrow TiO_2 + {}^{\bullet}OH_{ad} + H^+ \quad (7)$$

$$TiO_2(h^+) + {}^-OH_{ad} \rightarrow TiO_2 + {}^{\bullet}OH_{ad} \quad (8)$$

$$TiO_2(e^-) + O_2 \rightarrow TiO_2 + O_2^{\bullet -} \quad (9)$$

$$O_2^{\bullet -} + H_2O \rightarrow HO_2^{\bullet} + OH^- \quad (10)$$

$$2HO_2^{\bullet} \rightarrow O_2 + H_2O_2 \quad (11)$$

$$TiO_2(e^-) + H_2O_2 \rightarrow TiO_2 + {}^-OH + {}^{\bullet}OH \quad (12)$$

It has been shown in heterogeneous photocatalysis that, the addition of hydrogen peroxide enhances the rate of photodegradation, probably via reaction (12). Organic compounds adsorbed onto, or very close to the titanium dioxide surface can react with generated hydroxyl radicals, resulting in oxidation. As for the UV/TiO_2 system, the generation of $^{\bullet}OH$ radicals can arise as a result of reduction of the positive holes in the TiO_2 surface by electron donating species such as H_2O and OH^- (Eqs. (7) and (8)). Another pathway for OH radical formation is shown in Eq. (12) where the electrons on the TiO_2 surface can react with H_2O_2 to produce both OH^- and OH radicals. In experiments involving the systems TiO_2/UV and H_2O_2/UV/TiO_2, the decrease of imazamox concentration after 15 min of photodegradation was 63% and 76%, respectively. A total reduction has been observed after 1 h of irradiation (Fig. 2c and d). Addition of H_2O_2 made the process even more effective, since H_2O_2 is an efficient electron scavenger and a source of $^{\bullet}OH$ radicals (Eq. (12)).

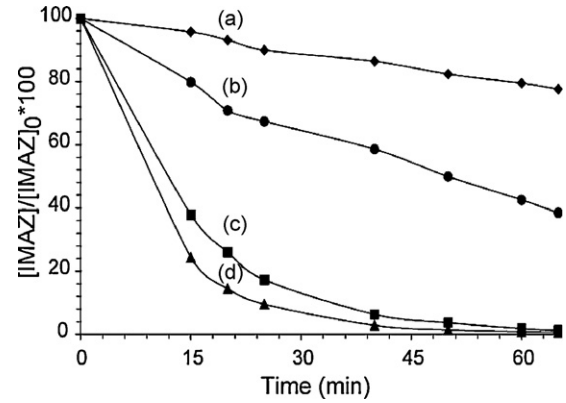

Fig. 2. Evolution curves of photocatalytic degradation of imazamox as a function of irradiation time; (a) IMAZ/UV, (b) H_2O_2/IMAZ/UV, (c) TiO_2/IMAZ/UV and (d) H_2O_2/TiO_2/IMAZ/UV; conditions: [IMAZ] = 0.065 mM, 10 mM H_2O_2, 1 g/l TiO_2 and natural pH.

3.2. Effect of titanium dioxide doses

The effect of TiO_2 P-25 amount in the aqueous solution on the observed photodegradation rate of imazamox is presented in Fig. 3. Different amounts of the catalyst ranging from 0.1 to 2 g/L and two concentration of the substrate (0.032 and 0.2 mM) were employed in this study. The initial reaction rate constants were calculated by the linear fit of each logarithmic degradation curve taking into account only the experimental data that were obtained during the first hour of reaction (in order to avoid the effect of the reaction intermediates).

It is clear from the preliminary investigations that catalyst loading is an important factor that can significantly influence the photocatalytic degradation of imazamox. Hence, the results obtained for both presented substrate concentrations reveal that, the reaction rate constant increases with the increase of the catalyst's amount up to a level which corresponds to the optimum of light absorption. This means, that excess of substrate with low

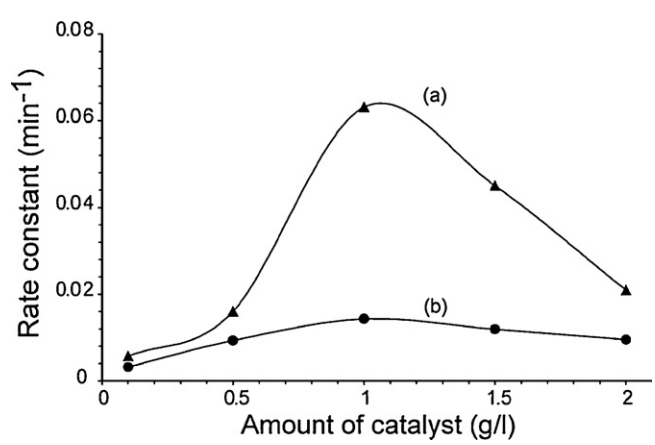

Fig. 3. The pseudo-first-order photo-decay of imazamox at various dosages of TiO_2 P-25; (a) 0.032 mM and (b) 0.2 mM concentrations of imazamox; 30 °C; natural pH.

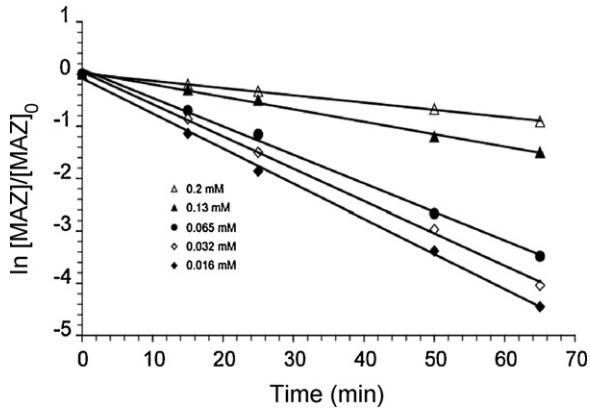

Fig. 4. Effect of initial imazamox concentration on the removal efficiency: the plot of $\ln[IMAZ]/[IMAZ]_0$ versus irradiation time.

amount of TiO_2 oversaturates the TiO_2 surface and therefore reduces the catalyst's efficiency. On the other hand, at overdoses of TiO_2, the intensity of the incident UV light was attenuated because of reduced light penetration and increased light scattering [23,33,34]. For both substrate concentrations, the maximum degradation rate constant was observed at a catalyst amount of 1 g/L, which was selected for the entire further studies.

3.3. Effect of the concentration

According to previous studies, the influence of the initial concentration of the solute on the photocatalytic degradation rate of the most organic compounds is described by pseudo-first-order kinetics which is rationalized in terms of the Langmuir–Hinshelwood model, modified to accommodate reactions occurring at a solid–liquid interface [35–38]. Hence, the effect of imazamox concentration was investigated in the presence of 1 g/L of TiO_2 in the substrate concentration range of 0.016–0.2 mM. Fig. 4 shows that the degradation rate decreases as the initial imazamox concentration increases. This observation is in agreement with the case of imazaquin and imazethapyr [23,34]. The imazamox kinetics degradation is not simple first-order but pseudo first-order.

The Langmuir–Hinshelwood kinetic expression has been used for heterogeneous photocatalysis to describe the relationship between the initial degradation rate and the initial concentration [37–42]. In this model, the reaction rate for second-order surface decomposition of IMAZ is written as follows:

$$r = -\frac{d[IMAZ]}{dt} = k_r \frac{k_{IMAZ}[IMAZ]}{1 + k_{IMAZ}[IMAZ]_0} \quad (13)$$

where [IMAZ] is the imazamox concentration at time t, k_r is the second-order rate constant, k_{IMAZ} is the equilibrium adsorption constants of imazamox onto TiO_2, and $[IMAZ]_0$ is the initial concentration of imazamox. According to Eq. (13), the photocatalytic degradation of imazamox in the presence of TiO_2 exhibits pseudo first-order kinetics with respect to imazamox concentration as in

$$-\frac{d[IMAZ]}{dt} = k_{obs}[IMAZ] \quad (14)$$

$$k_{obs} = k_r \frac{k_{IMAZ}}{1 + k_{IMAZ}[IMAZ]_0} \quad (15)$$

where k_{obs} is the observed pseudo first-order rate constant for the photocatalytic oxidation of imazamox (Eq. (15)). The integration of Eq. (14) results in

$$\ln\left(\frac{[IMAZ]_0}{[IMAZ]}\right) = k_{obs}t \quad (16)$$

According to Eq. (16), the straight-line relationship of $\ln[IMAZ]/[IMAZ]_0$ versus irradiation time was observed as indicated in Fig. 4.

The relationship between k_{obs} and $[IMAZ]_0$ can be expressed by Eq. (17)

$$\frac{1}{k_{obs}} = \frac{1}{k_r k_{IMAZ}} + \frac{[IMAZ]_0}{k_r} \quad (17)$$

Eq. (17) shows that the linear expression also can be obtained by plotting the reciprocal of degradation rate constant ($1/k_{obs}$) as a function of the initial imazamox concentration. Based on this equation, the values of k_{obs} at different initial imazamox concentration were fitted, and plotted in Fig. 5. By means of a least square best fitting procedure, the values of the adsorption equilibrium constant (k_{IMAZ}), and the second-order rate constant (k_r) were obtained, and these values are found to be k_{IMAZ} = 83.37 mM^{-1} and k_r = 0.0031 mM min (r^2 = 0.9845).

3.4. Effect of addition of hydrogen peroxide

The effect of adding H_2O_2 on the photolysis degradation rates of imazamox was examined by applying four different H_2O_2 concentrations without the use of TiO_2. Each concentration was increased by a factor of five in order to examine the effect of concentration clearly (Fig. 6) shows the degradation of imazamox at different concentrations of H_2O_2 under UV irradiation. Increasing H_2O_2 concentration from 5 to 10 mM increased the degradation rate of imazamox. Further increase of H_2O_2 concentration (over 10 mM) decreased photo-degradation efficiency of imazamox. It has been observed that, in aqueous phase, the combination of H_2O_2 and UV radiation has proved to enhance degradation rates when compared to UV irradiation with absence of H_2O_2. Photo-decomposition of H_2O_2 results in formation of $^{\bullet}OH$ which are very reactive radical species and attack the organic compounds (Eq. (18)) [43,44]. Increase in H_2O_2 concentration has been reported to enhance the reaction rate to a specific limit. However, when the reaction rate reached a maximum, further addition of more H_2O_2 inhibited the reaction. It has been suggested that, hydroxyl radicals can reversely recombine into hydrogen peroxide and an excess of spiked H_2O_2 likely acts as $^{\bullet}OH$ scavenger to produce much less reactive hydroperoxyl radical (Eq. (19)), which consequently causes the decrease of the initial reaction rates

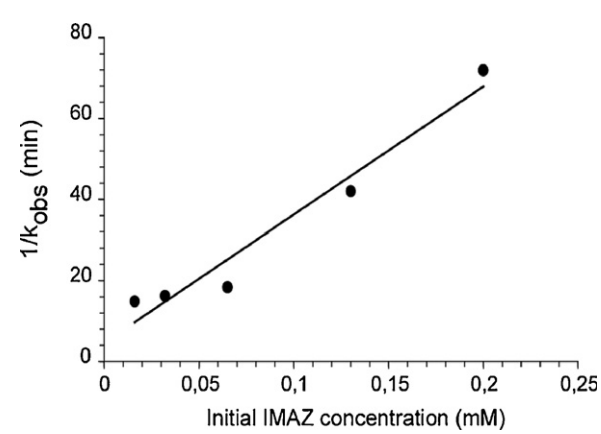

Fig. 5. Plot of the initial imazamox concentration versus the reciprocal of the observed first-order rate constant ($1/k_{obs}$).

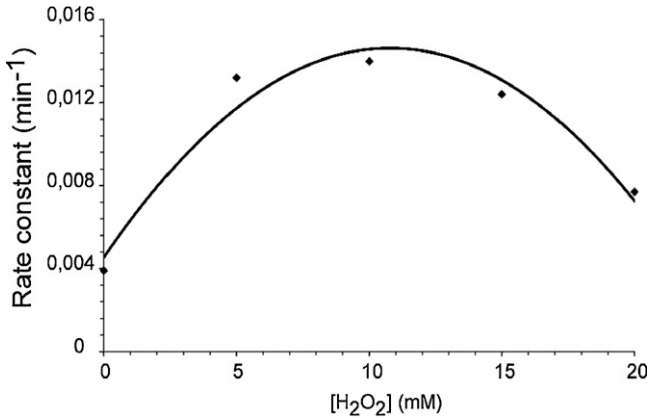

Fig. 6. Effect of H_2O_2 concentration on the photo-degradation rate of imazamox (0.065 mM of imazamox; 30 °C; natural pH). No TiO_2 was used in this experiment.

(Eq. (22)) [43–46]. The optimum concentration of H_2O_2 is 10 mM for the abatement of imazamox.

$$H_2O_2 + h\nu \rightarrow {}^{\bullet}OH + {}^{\bullet}OH \quad (18)$$

$${}^{\bullet}OH + H_2O_2 \rightarrow H_2O + HO_2{}^{\bullet} \quad (19)$$

$$HO_2{}^{\bullet} + H_2O_2 \rightarrow H_2O + O_2 + {}^{\bullet}OH \quad (20)$$

$$HO_2{}^{\bullet} + HO_2{}^{\bullet} \rightarrow H_2O_2 + O_2 \quad (21)$$

$${}^{\bullet}OH + HO_2{}^{\bullet} \rightarrow H_2O + O_2 \quad (22)$$

3.5. Effect of pH

It is known that the pH of the reaction medium has a significant effect on the surface properties of the TiO_2 catalyst, which include the surface charge of the particles, the size of the aggregate of catalyst particles it forms, and the band edge position of TiO_2. The surface of the photocatalyst can be protonated in acidic and deprotonated in alkaline medium as shown in following equations:

$$Ti^{IV}OH + H^+ \Leftrightarrow Ti^{IV}OH_2{}^+ \quad (23)$$

$$Ti^{IV}OH + OH^- \Leftrightarrow Ti^{IV}O^- \quad (24)$$

The point of zero charge (pzc) of TiO_2 P-25 is reported at pH ~6.25 [47]. Thus, the TiO_2 surface will remain positively charged in acidic medium (pH < 6.25) and negatively charged in alkaline medium (pH > 6.25). This behaviour affects the adsorption and desorption properties of TiO_2. Furthermore, the structures of the pollutants change with the pH, depending on the availability of ionisable organic functional groups, which can be protonated or deprotonated in dependence of the pH of the solution.

Imazamox is an amphoteric herbicide, which posses a carboxylic acid and a basic pyridine functional group. The dissociation constant (pK_a) of this herbicide were calculated with Pallas 3.1 (CompuDrug International Inc, Budapest, Hungary) and values found were $pK_{a1} = 2.09$ and $pK_{a2} = 5.04$ corresponding to the carboxylic acid and pyridine, respectively. The calculated values of both pK_a values were less than 6 resulting in the predominance of the anionic form of the herbicide above pH 6.

The imazamox degradation rate was investigated by stirring the aqueous solution of herbicide under simulated sunlight irradiation at different pH values ranging from pH 2 to pH 11. Results obtained are illustrated in Table 1. In highly acidic medium, the degradation rate is low and it increases, as the pH increases up to pH value ~5.0 (Table 1). Above this value, the degradation rate decreases, indicating that the pH can affect significantly the corresponding degradation rate of imazamox. Due to the electrostatic effects, the anionic imazamox form adsorbs on the positively charged surface of the catalyst ($TiOH_2{}^+$) at pH~5.0, leading to an increase in degradation rate. Consequently, at higher and lower pH values, the decrease in degradation rate is attributed to the anion–anion and cation–cation repulsion, respectively, which occur between the charged herbicide and the charged catalyst surface.

Table 1
Rate constant of imazamox degradation at different pH values (0.065 mM; m(TiO_2) = 1 g/L; 30 °C)

pH	k ($\times 10^{-2}$ min^{-1})	$t_{1/2}$ ($\times 10^2$ min)	r^2
2.04	0.16	4.331	0.9932
3.01	0.50	1.386	0.9948
4.08	1.56	0.444	0.9963
5.03	6.71	0.103	0.9991
7.18	5.37	0.129	0.9971
8.1	5.35	0.129	0.9911
9.13	5.45	0.127	0.9934
10.05	3.02	0.229	0.9929
11.03	0.90	0.770	0.9951

Fig. 7 shows the DFT optimized geometries of imazamox neutral and its corresponding anion and cation. These geometries correspond to energy minima without PCM (polarizable continuum model) correction. Mulliken charge distributions on hetero-atoms are given in Fig. 7. Table 2 lists Mulliken partial charges of important constituents of imazamox. It can be concluded that terminal ether has a partial repulsion effect only in the anionic structure. The carboxyl group does not play the whole role in establishing an anion–anion columbic repulsion between imazamox anion and TiO^-. The ether terminal and the C–N–C edge bear significant partial negative charge in the anionic form of imazamox. Thus, there are three partial negative centers located in different positions in imazamox, which repel the anion from TiO^- surface.

The cation–cation interaction has a higher repulsion effect than the anion–anion interaction as can be deduced from Table 2. The cation–cation repulsion is higher not only because the positive charge is delocalized on the pyridine surface with high cross-section but also because the dihedral angle CC {pyridine}–CN {imidazol} in the cationic form of imazamox is nearly zero (Table 2). This positions both pyridine and imidazol rings in the same plane. Thus, cation–cation repulsion between the positively charged pyridine ring and $TiOH^+$ repel the whole imazamox cation and does not let the imidazol ring to be attracted into the catalyst surface. Therefore, we conclude that the rate decrease for pH values lower or higher than 5 is not only due to the partial charge distribution of imazamox but also to the conformational

Table 2
Sum of atomic partial charges on specific groups in imazamox and their calculated dihedral angles in different structures

Moiety	Imaz$^+$	Imaz$^\pm$	Imaz$^-$
CH_3	0.215	0.155	0.042
$CH_2(CH_3)_2$	0.388	0.124	0.144
C(O)-NH- in imidazol	0.043	0.059	0.069
C-N-C in imidazol	−0.738	−0.501	−0.482
Pyridine	0.803	0.235	0.046
Carboxyl group	0.182	−0.013	−0.431
Terminal ether	0.107	−0.06	−0.387
Sum of partial charges	1.000	−0.001	−0.999
Dihedral angle CC{py}-CN{imidazol}	0.09	−81.2	31.4

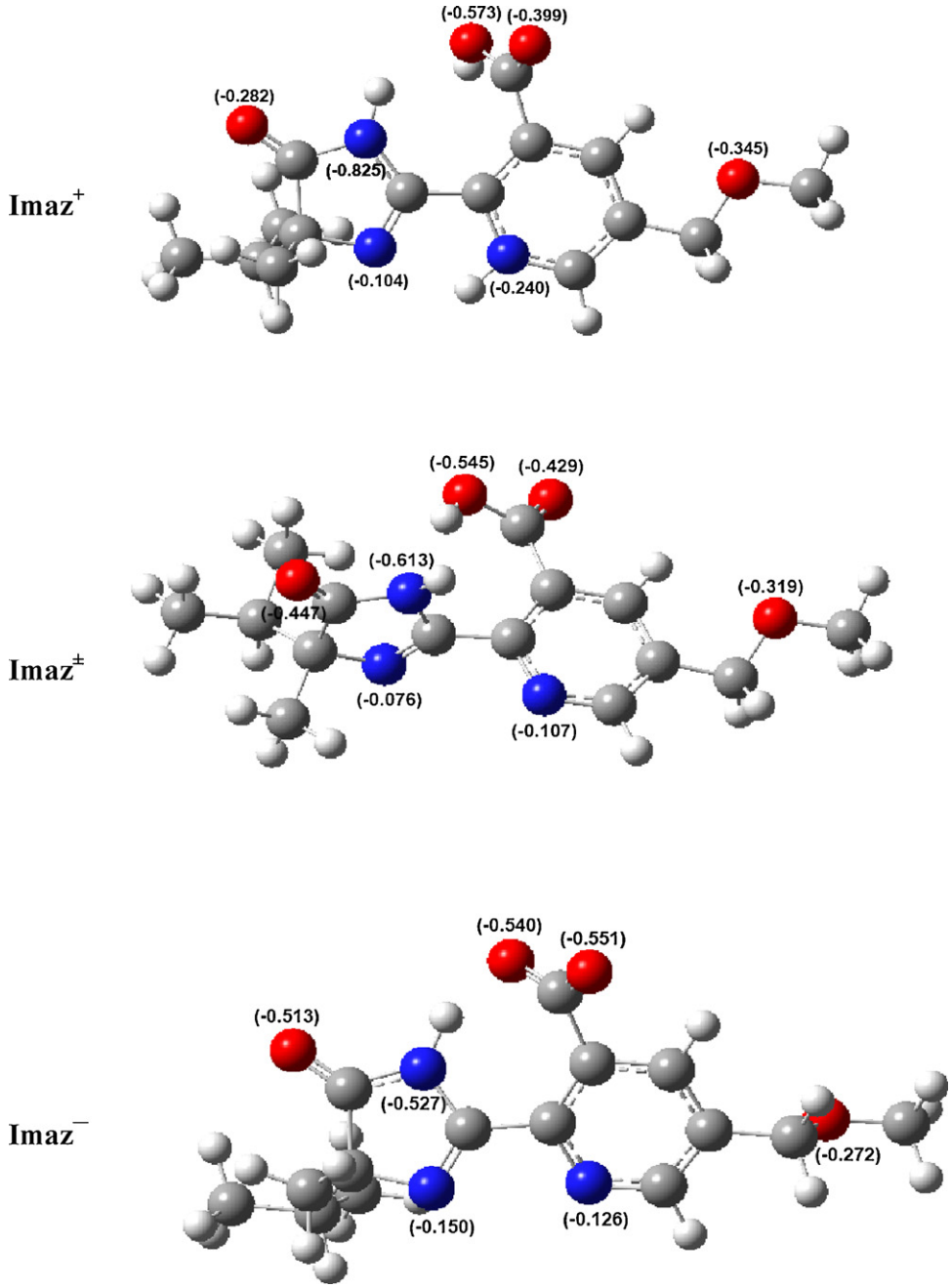

Fig. 7. Partial charge densities of heteroatoms in ionized and neutral imazamox.

changes that imazamox undergoes through ionization, which is pH dependent.

To sum up, these results confirm the links between adsorption of the substrate on the catalyst surface and the degradation rate. It indicates further that the photo-catalytic degradation is surface phenomenon. Similar behaviour was observed in the cases of imazapyr, imazethapyr and imazaquin [16,23,34].

3.6. Identification of photo-products

The data obtained for the photodegradation of imazamox is shown in Table 3. The mass spectra and proposed structures are shown in Figs. 8 and 9. According to previous studies [48,49], the characterization of the main photoproducts were investigated based on their accurate mass measurements and their proposed chemical structure.

Electrospray ionization in positive mode coupled to FT-ICR measurements revealed the presence of five photoproducts (Fig. 8A, 9A and Fig. 8b, 9b) attributed as following: the peak at $m/z = 292.129$ corresponds to the formula $C_{14}H_{18}N_3O_4$, and was attributed to product 1 (Table 3) as a result of rupture of the methoxy group. The next peak ($m/z = 278.149$, $C_{14}H_{20}N_3O_3$) is a product formed by decarbonylisation of the carboxyl group in imazamox, and is labeled 2 in Table 3. The product $m/z = 263.138$ corresponds to $C_{14}H_{19}N_2O_3$ and is assigned to structure 3 (Table 3) formed by rearrangement of the proton in α-position of the imidazole ring by loss of HNCO. The peak at m/z 211.071, corresponds to the sum formula $C_9H_{11}N_2O_4$ (structure 4 in

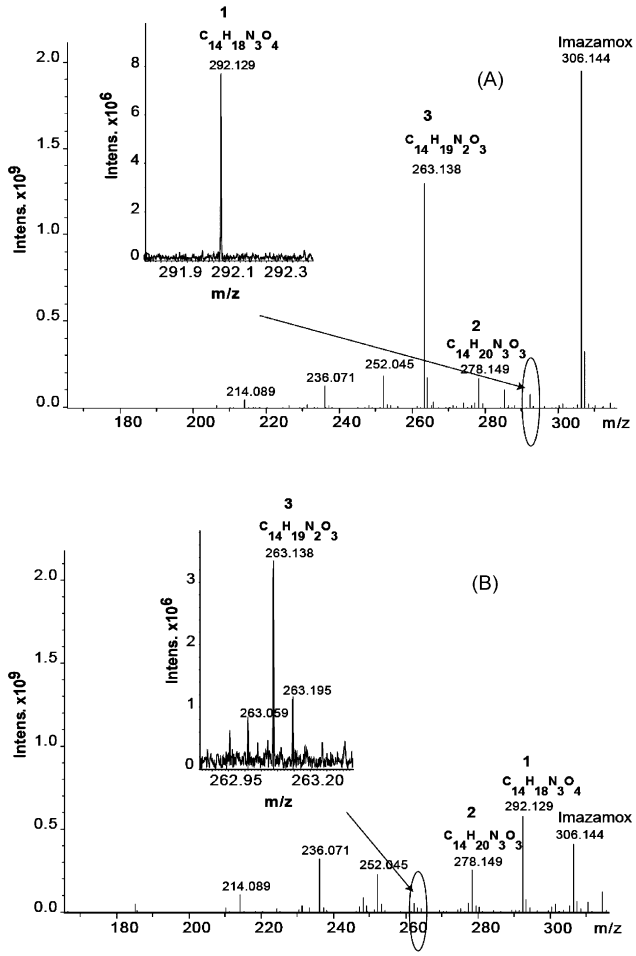

Fig. 8. FT-ICR mass spectra of imazamox photodegradation (A: In absence of H_2O_2, B: in presence of H_2O_2). Inserts represent an enlarged view of the specific identified photo-degradation products on the mass scale.

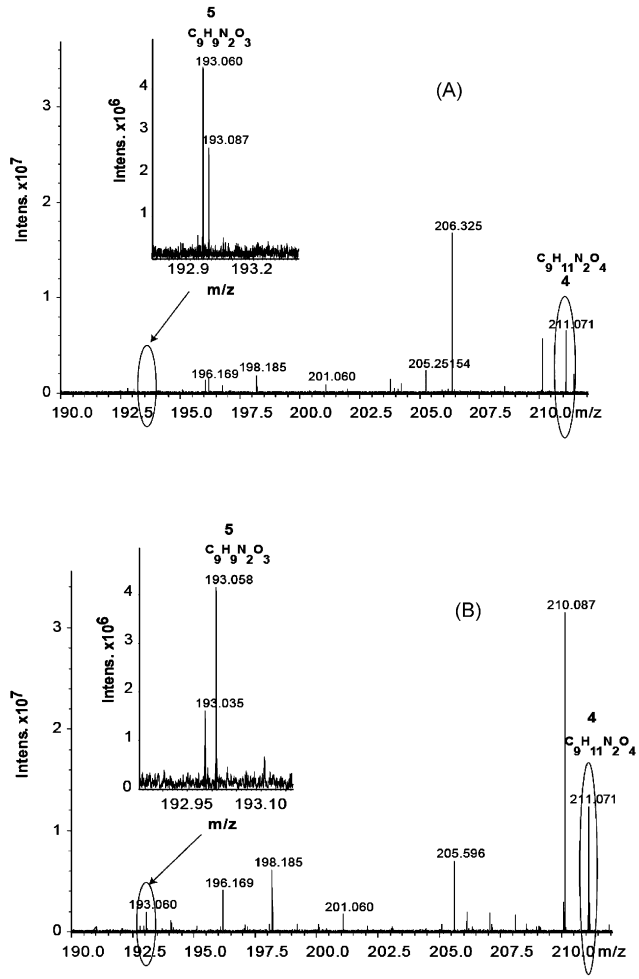

Fig. 9. Enlarged mass scale of imazamox spectrum in the region m/z = (190–212) Da. (A: In absence of H_2O_2, B: in presence of H_2O_2).

Table 3
Imazamox and its degradation products as detected by ESI FT-ICR-MS in positive ionization mode (in absence and presence of H_2O_2)

Chemical structure	Name	Measured mass	Error (ppm)	$[M+H]^+$
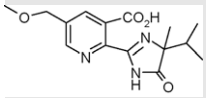	**Imazamox**: 2-(4-isopropyl-4-methyl-5-oxo-4,5-dihydro-1H-imidazol-2-yl)-5-(methoxymethyl)nicotinic acid	306.144	0.054	$C_{15}H_{20}N_3O_4$
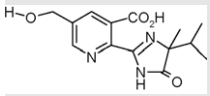	(**1**): 5-(hydroxymethyl)-2-(4-isopropyl-4-methyl-5-oxo-4,5-dihydro-1H-imidazol-2-yl)nicotinic acid	292.129	0.217	$C_{14}H_{18}N_3O_4$
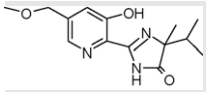	(**2**): 2-(3-hydroxy-5-(methoxymethyl)pyridin-2-yl)-4-isopropyl-4-methyl-1H-imidazol-5(4H)-one	278.149	0.040	$C_{14}H_{20}N_3O_3$
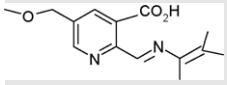	(**3**): (*E*)-5-(methoxymethyl)-2-((3-methylbut-2-en-2-ylimino)methyl)nicotinic acid	263.138	0.003	$C_{14}H_{19}N_2O_3$
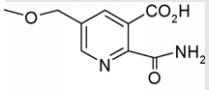	(**4**): 2-Carbamoyl-5-(methoxymethyl)nicotinic acid	211.071	0.067	$C_9H_{11}N_2O_4$
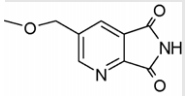	(**5**): 3-(methoxymethyl)-5H-pyrrolo[3,4-b]pyridine-5,7(6H)-dione	193.060	0.047	$C_9H_9N_2O_3$

(**1**), (**2**), (**3**), (**4**) and (**5**): See Figs. 8 and 9(A and B).

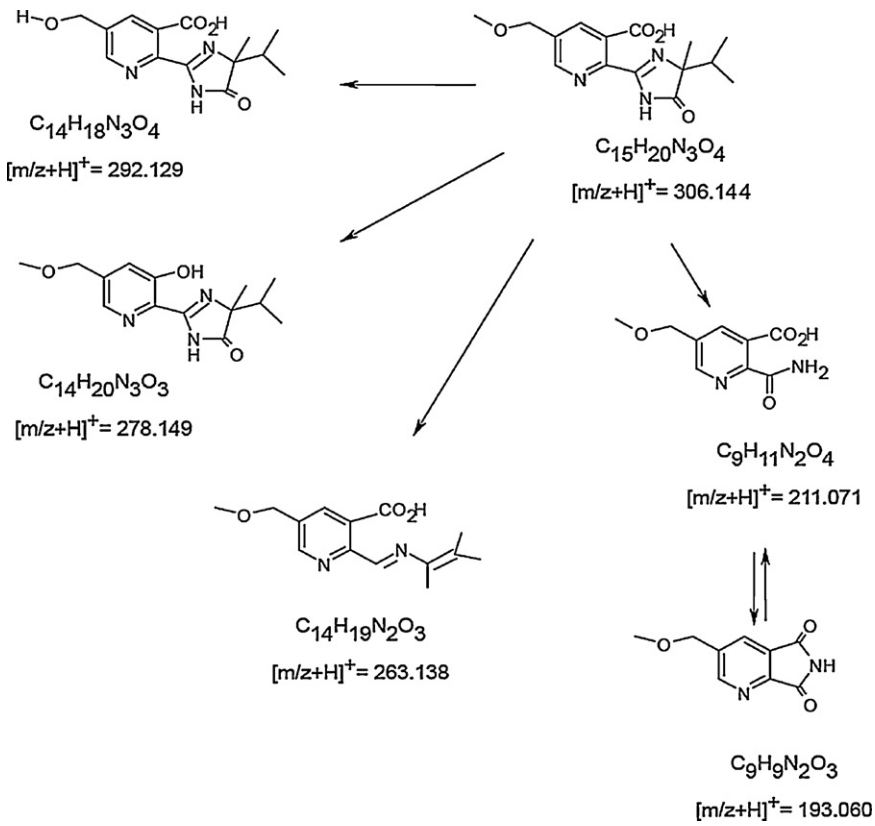

Fig. 10. Scheme of global proposal of photoproducts pathways of imazamox photodegradation.

Table 3). As a result of loss of one water molecule, we can succeed to the condensation process between both the amide and carboxyle groups leading to structure 5 $m/z = 193.060$ ($C_9H_9N_2O_3$), which could be explained by Nourish reaction.

To sum up, the photodecomposition of imazamox in the homogeneous reaction takes place only on imidazole ring leading to three sequential degradation steps: decarbonylisation (CO removal), cleavage of carbon-heteroatom bond and rearrangement. On the basis of both the proposed structural information of the corresponding detected sum formulas obtained from FT-ICR mass spectra for photodegradation of imazamox and the known photo-induced reactions found in the literature [25,48–50], a tentative photodegradation scheme is proposed in Fig. 10.

4. Conclusion

Photodegradation of imazamox herbicide was studied at different photocatalytic processes by using TiO_2 P-25 as catalyst. The results obtained are as follow:

- The degradation rates were always higher for heterogeneous photocatalysis as compared to non-catalytic reactions. Imazamox degradation followed a pseudo first-order rate expression according to the Langmuir–Hinshelwood kinetic model.
- Photocatalytic degradation rates increased with TiO_2 amount, but overdoses may cause rate retardation because the effect of light scattering becomes significant. The degradation rate also increases with an increase in H_2O_2 concentration. Furthermore, the degradation rate was retarded over catalyst concentration of 10 mM. On the other hand, at alkalic and low acidic conditions, the degradation of imazamox showed lower photocatalytic degradation efficiency. The optimum values for the abatement of this herbicide were found to be: pH (~5.0), 1 g/L (TiO_2) and 10 mM of H_2O_2.
- Mulliken charge distribution and conformational properties change between the cationic, anionic and neutral forms of the herbicide. These changes elucidate detailed information in regard to the herbicide interaction with the charged surface of the catalyst.
- In this study, FT-ICR Mass Spectrometry was involved as a new tool for identification and characterisation of the degradation products.

Acknowledgments

The authors thank the German Academic Exchange Service (DAAD) for a grant to MH and the German–Israeli Foundation for Scientific Research and Development (GIF) for financial support of MH and MF.

References

[1] P.C. Zhang, R.J. Scrudato, J.J. Pagano, R.N. Roberts, Chemosphere 26 (1993) 1213.
[2] J. Chiarenzelli, R. Scrudato, M. Wunderlich, D. Raerty, K. Jensen, G. Oenga, R. Roberts, J. Pagano, Chemosphere 31 (1995) 3259.
[3] I.W. Huang, C.S. Hong, B. Bush, Chemosphere 32 (1996) 1869.
[4] S. Wen, J. Zhao, G. Sheng, J. Fu, P. Peng, Chemosphere 50 (2003) 111.
[5] I. Poulios, M. Kositzi, A. Kouras, J. Photochem. Photobiol. A 115 (1998) 175.
[6] G.A. Peñuela, D. Barceló, J. AOAC Int. 83 (2000) 53.
[7] H. Hidaka, K. Nohara, J. Zhao, K. Takashima, E. Pelizzetti, N. Serpone, New J. Chem. 18 (1994) 541.
[8] Y. Wang, C.S. Hong, F. Fang, Environ. Eng. Sci. 16 (1999) 433.
[9] Q. Huang, C.S. Hong, Chemosphere 41 (2000) 871.
[10] T.T. Clive, The Pesticide Manual, 10th ed., Crop Protection Publication, the Royal Society of Chemistry (1995).
[11] C.A. Reyes, M. Medina, C.Z. Hernandez, M.Z. Cedeno, R. Arce, O. Rosario, D.M. Steffenson, I.N. Ivanov, M. Sigman, R. Dabestani, Chemosphere 34 (2000) 415.
[12] M.E. Sigman, P.F. Schuler, M.M. Ghosh, J. Photochem. Photobiol. A 32 (1998) 3980.

[13] H. Hidaka, T. Shimura, K. Ajisaka, S. Horikoshi, J. Zhao, N. Serpone, J. Photochem. Photobiol. A 109 (1997) 165.
[14] R.B. Draper, M.A. Fox, Phys. Chem. 94 (1990) 4628.
[15] E. Quivet, R. Faure, J. Georges, J.-O. Païssé, B. Herbreteau, P. Lantéri, J. Agric. Food Chem. 54 (2006) 3641–3645.
[16] J.A. Osajima, H.M. Ishiki, K. Takashima, Monatsh. Chem. 139 (2008) 7–11.
[17] M. Brigante, C. Emmelin, C. Ferronato, M.D. Greca, L. Previtera, J.O. Paisse, J.-M. Chovelon, Chemosphere 68 (2007) 464–471.
[18] M. Mekkaoui, M. El Azzouzi, A. Bouhaouss, M. Ferhat, A. Dahchour, S. Guittonneau, Meallier, Fresenius Environ. Bull. 9 (2000) 783.
[19] M. El Azzouzi, H. Mountacer, M. Mansour, Fresenius Environ. Bull. 8 (1999) 709.
[20] H.D. Burrows, L.M. Canle, L.J.A. Santaballa, S. Steenken, J. Photochem. Photobiol. B: Biol. 67 (2002) 71.
[21] W.S. Curran, M.M. Loux, R.A. Liebl, F.W. Simmons, Weed Sci. 40 (1992) 143.
[22] G. Mangels, in: D.L. Shaner, S.L. O'Connor (Eds.), The Imidazolinone Herbicides, CRC Press, Boca Raton, FL, 1991 , p. 290 (Chapter 16).
[23] J.C. Garcia, K. Takashima, J. Photochem. Photobiol. A Chem. 155 (2003) 215.
[24] P. Pizarro, C. Guillard, N. Perol, J.-M. Herrmann, Catal. Today 101 (2005) 211.
[25] M. Carrier, N. Perol, J.-M. Herrmann, C. Bordes, S. Horikoshi, J.O. Paisse, R. Budot, C. Guillard, Appl. Catal. B Environ. 65 (2006) 11–20.
[26] M.J. Frisch, G.W. Trucks, H.B. Schlegel, G.E. Scuseria, M.A. Robb, J.R. Cheeseman, J.A. Montgomery, Jr., T. Vreven, K.N. Kudin, J.C. Burant, J.M. Millam, S.S. Iyengar, J. Tomasi, V. Barone, B. Mennucci, M. Cossi, G. Scalmani, N. Rega, G.A. Petersson, H. Nakatsuji, M. Hada, M. Ehara, K. Toyota, R. Fukuda, J. Hasegawa, M. Ishida, T. Nakajima, Y. Honda, O. Kitao, H. Nakai, M. Klene, X. Li, J.E. Knox, H.P. Hratchian, J.B. Cross, V. Bakken, C. Adamo, J. Jaramillo, R. Gomperts, R.E. Stratmann, O. Yazyev, A.J. Austin, R. Cammi, C. Pomelli, J.W. Ochterski, P.Y. Ayala, K. Morokuma, G.A. Voth, P. Salvador, J.J. Dannenberg, V.G. Zakrzewski, S. Dapprich, A.D. Daniels, M.C. Strain, O. Farkas, D.K. Malick, A.D. Rabuck, K. Raghavachari, J.B. Foresman, J.V. Ortiz, Q. Cui, A.G. Baboul, S. Clifford, J. Cioslowski, B.B. Stefanov, G. Liu, A. Liashenko, P. Piskorz, I. Komaromi, R.L. Martin, D.J. Fox, T. Keith, M.A. Al-Laham, C.Y. Peng, A. Nanayakkara, M. Challacombe, P.M.W. Gill, B. Johnson, W. Chen, M.W. Wong, C. Gonzalez, J.A. Pople, Gaussian 03, Revision D, Gaussian, Inc., Wallingford, CT, 2004.
[27] H.B. Schlegel, J. Comput. Chem. 2 (1982) 214–218.
[28] P. Csaszar, P. Pulay, J. Mol. Struct. 114 (1984) 31–34.
[29] O. Farkas, H.B. Schlegel, Phys. Chem. 1 (2002) 11–15.
[30] O. Farkas, H.B. Schlegel, J. Chem. Phys. 24 (1999) 10806–10814.
[31] R. Dennington II, T. Keith, J. Millam, K. Eppinnett, W.L. Hovell, R.Gilliland, GaussView, Version 3.0.9, Semichem, Inc., Shawnee Mission, KS, 2003.
[32] O. Legrini, E. Oliveros, A.M. Braun, Chem. Rev. 93 (1993) 671–698.
[33] C.C. Wong, W. Chu, Chemosphere 50 (2003) 981–987.
[34] R.R. Ishiki, H.M. Ishiki, K. Takashima, Chemosphere 58 (2005) 1461–1469.
[35] C.S. Turchi, D.F. Ollis, J. Catal. 122 (1990) 178–192.
[36] H. Al-Ekabi, N. Serpone, J. Phys. Chem. 92 (1988) 5726–5731.
[37] J. Cunningham, G. Al-sayyed, P. Sedlak, J. Caffrey, Catal. Today 53 (1999) 145–158.
[38] R.W. Matthews, J. Catal. 111 (1988) 264–270.
[39] M.C. Lu, G.D. Roam, J.N. Chen, C.P. Huang, J. Photochem. Photobiol. A Chem. 76 (1993) 103–110.
[40] G. Mills, M.R. Hoffmann, Environ. Sci. Technol. 27 (1993) 1681–1689.
[41] D. Chen, A.K. Raym, Water Res. 32 (1998) 3223–3234.
[42] K. Chiang, T.M. Lim, L. Tsen, C.C. Lee, Appl. Catal. A, Gen. 261 (2004) 225.
[43] M. Anbar, P. Neta, Int. J. Appl. Radiat. Isot. 18 (1967) 493–523.
[44] F. Habber, R. Willstatter, Ber. Dtsch. Chem. Ges. 64 (1931) 2844.
[45] G.E. Adams, J.W. Boag, B.D. Michael, Proc. Royal Soc. 289 (1966) 321–341.
[46] J.L. Weeks, M.S. Matherson, J. Am. Chem. Soc. (1968) 1273–1278.
[47] J. Augustynski, Structure and Bonding, Springer, Berlin, New York, 1988, p. 69.
[48] M. Harir, M. Frommberger, A. Gaspar, D. Martens, A. Kettrup, M.El. Azzouzi, Ph. Schmitt Kopplin, Anal. Bioanal. Chem. 389 (2007) 1459–1467.
[49] M. Harir, A. Gaspar, M. Frommberger, M. Lucio, D. Martens, A. Kettrup, M. El Azzouzi, Ph. Schmitt-Kopplin, J. Agric. Food Chem. 55 (2007) 9936–9943.
[50] E. Quivet, R. Faure, J.J. Georges, Chem. Crystallogr. 34 (2004) 25.